Research Article / Review Article

FUPRE JOURNAL 9(4):259-275(2025)
DOI: /10.60787/FJSIR.v9i5.259-275

FUPRE Journal

of

Scientific and Industrial Research

ISSN: 2579-1184(Print) ISSN: 2578-1129 (Online)

http://fupre.edu.ng/journal

Green Synthesis of Biomass-Derived Nanocoagulants from Moringa oleifera 1 Husks and Carica papaya Seeds for Efficient Industrial Wastewater

***MBAH, J. C.*[1,*], *ANIKE, O. H.*[2]**

[1]*University of Delta, Agbor, Delta State, Nigeria*

[2]*University of Pardubice, Pardubice, Czech Republic*

ARTICLE INFO

Received: 21/10/2025
Accepted: 22/12/2025

Keywords

Biomass-derived nanomaterials, Carica papaya, Coagulation-flocculation, Green synthesis, Industrial wastewater treatment, Moringa oleifera

ABSTRACT

This research explores the green synthesis and application of nanomaterials derived from Moringa oleifera husks and Carica papaya seeds as sustainable nanocoagulants for treating industrial wastewater. These agricultural residues were transformed into nanoscale materials using eco-friendly methods and characterized for surface chemistry, particle size, and functional group distribution through FTIR, SEM, and BET analyses. Their coagulation-flocculation performance was evaluated on brewery and textile wastewater samples from Anambra State, Nigeria. Post-treatment analyses demonstrated substantial reductions in turbidity (up to 92.4%), total suspended solids (TSS, up to 88.1%), and chemical oxygen demand (COD, up to 76.3%), with Moringa oleifera husk nanoparticles (MOHNPs) outperforming Carica papaya seed nanoparticles (CPSNPs). Compared to bulk biomass, the nanomaterials exhibited superior pollutant removal efficiency and maintained near-neutral pH levels, reducing the need for additional neutralization. These findings highlight the potential of biomass-derived nanomaterials as cost-effective, eco-friendly alternatives to conventional coagulants, promoting sustainable wastewater management and agricultural waste valorization.

1. INTRODUCTION

The rapid ascent of industrialization and urbanization has significantly amplified the generation of complex wastewater streams, posing substantial threats to environmental integrity, biodiversity, and human health (Rahman *et al.*, 2021; Wei *et al.*, 2025). According to Precedence Research (2025), the global industrial wastewater treatment market was valued at USD 18.28 billion in 2024 and is projected to reach USD 34.11 billion by 2034, reflecting the growing demand for advanced remediation strategies like nanofiltration to address escalating pollution concerns (Precedence Research, 2025). However, global treatment coverage remains inadequate; approximately 30–40% of industrial wastewater is treated, with only a fraction achieving safe standards, leading to widespread contamination of aquatic ecosystems, freshwater scarcity, and

*Corresponding author, e-mail: juliet.mbah@unidel.edu.ng
DIO: /10.60787/FJSIR.v9i5.259-275
©Scientific Information, Documentation and Publishing Office at FUPRE Journal

bioaccumulation of toxins (UN-Water, 2023; Wang *et al.*, 2025). Industries such as brewing and textiles, with high-volume discharges rich in organic and inorganic pollutants, are major contributors to these environmental challenges (Das and Mishra 2025).

Brewery wastewater, characterized by high organic loads such as fermentable sugars, proteins, yeast residues, and elevated biochemical oxygen demand (BOD, 500–3,000 mg/L), poses significant environmental risks if discharged untreated (Kanagasubbulakshmi *et al.*, 2017, Simate *et al.*, 2011; Wang *et al.*, 2025). Untreated effluents can induce eutrophication in receiving water bodies, depleting dissolved oxygen, creating hypoxic zones, disrupting microbial communities, and promoting harmful algal blooms, while suspended solids and nutrients (nitrogen, phosphorus) contribute to groundwater contamination and long-term ecological imbalances, particularly in regions with inadequate treatment infrastructure (EPA 2025, *et al.*, 2023; UN-Water, 2023). Human health risks arise from potential contamination by pathogenic microorganisms in untreated brewery effluents, increasing the incidence of gastrointestinal illnesses upon exposure, though respiratory impacts are less documented (Simate *et al.*, 2011; Wei *et al.*, 2025).

Textile wastewater is characterized by a recalcitrant composition, including synthetic dyes, heavy metals (e.g., chromium, cadmium), surfactants, and chemical auxiliaries from dyeing and finishing operations, contributing to approximately 20% of global industrial water pollution (Mahdavi *et al.*, 2013, Holkar *et al.*, 2016; UNEP, 2016). Untreated discharges cause severe ecological disruptions, such as bioaccumulation in aquatic organisms, reduced photosynthetic activity due to light obstruction, and toxicity to fish and invertebrates (Ullah Bhat and Qayoom 2022, 2023; Wei *et al.*, 2025). Human exposure to textile wastewater contaminants, primarily through ingestion or dermal contact, is associated with carcinogenic effects (e.g., from benzidine-based azo dyes) and endocrine disruption (e.g., from phthalates), with potential organ damage to the liver and kidneys due to chronic exposure to heavy metals like chromium and cadmium (Holkar *et al.*, 2016; WHO, 2017). Immune system effects are less well-documented but plausible with prolonged exposure to organic pollutants. Respiratory impacts are negligible for wastewater exposure and are primarily associated with occupational inhalation of dye aerosols during textile processing (Holkar *et al.*, 2016). The alkaline pH (8–12) and high salinity (TDS 1,000–10,000 mg/L) of textile effluents, when used for irrigation, alter soil chemistry, reduce agricultural productivity, and contribute to land degradation (Rofiul and Rafiur 2025). These impacts necessitate compliance with stringent environmental regulations, such as those under the EU Water Framework Directive and regional discharge standards, to mitigate ecological and socio-economic consequences (UN-Water, 2023).

Coagulation-flocculation is a critical wastewater treatment technique, destabilizing colloidal particles and aggregating them into separable flocs to remove suspended solids (70–90%), colloids, and some dissolved organics (20–50% COD) from industrial effluents (Bratby, 2016; Wang *et al.*, 2025). However, traditional chemical coagulants like aluminum sulfate, ferric chloride, and polyaluminum chloride generate voluminous, non-biodegradable sludge (1–5 kg/m³), increasing disposal costs (0.05–0.2 €/m³) and environmental burdens (Vazquez-Muñoz *et al.*, 2019; Bhatt *et al.* 2022; Kim *et al.*, 2024). These coagulants are potentials for secondary contamination of

treated water, challenges associated with sludge management, and high operational costs that can burden industrial facilities (Yew *et al.*, 2016; Naganthran et al, 2022). These coagulants may introduce residual metals, such as aluminum (0.1–1 mg/L), which have been studied for potential neurotoxic effects at high exposure levels. However, the association with Alzheimer's disease is not supported by conclusive evidence at typical residual concentrations in treated water (Bondy, 2016). Additionally, pH adjustments (pH 6–8) increase chemical inputs and carbon footprints (0.1–0.2 kg CO_2eq/m³), while excessive sludge complicates wastewater management (Bratby, 2016). These limitations have spurred research into sustainable alternatives, such as bio-coagulants and electrocoagulation, to enhance efficacy and reduce ecological impacts (Kim *et al.*, 2024; Wei *et al.*, 2025).

Consequently, there has been a growing interest in exploring greener technologies that harness natural and renewable resources for wastewater treatment (Patave et al, 2018; Ahmed et al, 2016; Natarajan, 2017) as this technology is prominent in wastewater remediation, offering sustainable alternatives to conventional treatments (Crini and Lichtfouse, 2019; Wei *et al.*, 2025). Green synthesis of nanomaterials, using plant-based precursors, produces eco-friendly nanoparticles that valorize agricultural wastes, aligning with circular economy principles, and exhibit enhanced surface area (100–500 m²/g) and reactivity for superior adsorption and charge neutralization (Saratale *et al.*, 2018). *Moringa oleifera* husks, rich in cationic proteins, polyphenols, and polysaccharides, serve as effective natural coagulants, with nano-engineered forms achieving 80–90% turbidity and 50–80% heavy metal removal, surpassing bulk forms due to their fibrous, porous structure (Crini and Lichtfouse, 2019; Wei *et al.*, 2025). Similarly, *Carica papaya* seeds, containing positively charged proteins like papain, function as bio-coagulants, reducing turbidity and suspended solids (60–85%) in organic-rich effluents such as COD (500–2,000 mg/L), offering an eco-friendly solution for wastewater treatment (Simate *et al.*, 2011; Crini and Lichtfouse, 2019).

This study investigates the green synthesis, characterization, and efficacy of *Moringa oleifera* husk nanoparticles (MOHNPs) and *Carica papaya* seed nanoparticles (CPSNPs) in treating brewery and textile wastewater from Anambra State, Nigeria. Employing eco-friendly precipitation and milling protocols, the nanomaterials' performance will be assessed via metrics including turbidity, total suspended solids (TSS), chemical oxygen demand (COD), and pH stabilization. By delineating mechanisms of enhanced coagulation relative to conventional and bulk alternatives, this research aims to foster sustainable wastewater management, agricultural waste utilization, and accessible purification solutions in developing contexts.

2. MATERIALS AND METHOD

2.1 Wastewater Sampling

Wastewater samples from brewery and textile industries, as depicted in Figures 1 and 2, were collected from industrial facilities in Anambra State, Nigeria, specifically from a brewing facility's main discharge outlet and a textile plant's dyeing process drain, known for high concentrations of organic and chemical pollutants (e.g., dyes, heavy metals) (Holkar *et al.*, 2016; Simate *et al.*, 2011). Sampling followed standard protocols (APHA, 2017) to ensure representativeness and integrity. Composite samples (2 L per site) were collected over 24 h using automated samplers (ISCO 3700) at flow-proportional intervals to account for discharge variability. Brewery effluent was sampled post-fermentation, reflecting high

organic loads (COD 1029 mg/L), while textile effluent was collected post-dyeing, capturing recalcitrant compounds (COD 1890 mg/L). Samples were stored in pre-sterilized, high-density polyethylene containers, pre-rinsed with 1% HNO_3 and deionized water (18.2 MΩ·cm, Milli-Q), and maintained at 4-7 ℃ in a portable cooler during transport to prevent microbial degradation or chemical alteration. All analyses were conducted within 24 h of collection to preserve physicochemical properties, adhering to international guidelines for wastewater sampling (APHA, 2017; UN-Water, 2023). Triplicate samples were collected from each site to ensure reproducibility, with initial characterization (turbidity, TSS, COD, pH) performed to establish baseline pollutant levels prior to treatment.



Figure 1: Brewery wastewater before treatment



Figure 2: Textile wastewater before treatment

2.2 Biomass Collection and Nanomaterial Synthesis

Moringa oleifera husks and *Carica papaya* seeds, depicted in Figures 3 and 4, were sourced from local agricultural suppliers in Anambra State, Nigeria to ensure freshness and minimal contamination. Biomass was rigorously screened for impurities and washed with deionized water (18.2 MΩ·cm, Milli-Q) three times to remove surface contaminants, followed by air-drying at 25°C for 24 hour to preserve bioactive components. Subsequently, the biomass was oven-dried at 60°C for 12 h to reduce moisture content to <5% w/w, enhancing milling efficiency (Venkateswarlu et al, 2013; Sirdeshpandeet al, 2018, Simate *et al.*, 2011; Crini and Lichtfouse, 2019). The dried biomass was pulverized using a high-energy ball mill (LBM-1820-2) at 300 rpm for 30 min, achieving a particle size of 50–100 μm, verified by laser diffraction (Malvern Panalytical 2000) (Haque *et al.* 2017; Sudarman *et al.* 2023, Saratale *et al.*, 2018).

Nanoparticle synthesis followed a green chemistry protocol to minimize environmental impact. For *Moringa oleifera* husks, a chemical precipitation method was employed using aqueous husk extract (10 g/L, pH 7.0) as a reducing and capping agent, combined with 0.1 M metal salt solution ($Zn(NO_3)_2$) at a 1:1 v/v ratio under constant stirring (500 rpm, 60°C, 2 h). The resulting precipitate was filtered, washed with ethanol (95% v/v), and calcined at 400°C for 3 h in a muffle furnace to enhance crystallinity (Jadoun *et al.*, 2021, Roy *et al.*, 2015; Wei *et al.*, 2025). For *Carica papaya* seeds,

mechanical milling was followed by hydrothermal synthesis, where ground seed powder (5 g/L) was mixed with deionized water and autoclaved at 120°C and 15 psi for 4 h, producing nanoparticles with high cationic protein content (Saratale *et al.*, 2018). Both processes avoided toxic solvents, aligning with circular economy principles by valorizing agricultural waste. The synthesized nanomaterials were characterized using advanced analytical techniques to confirm their suitability for wastewater treatment. Fourier-transform infrared spectroscopy (FTIR, Agilent Technology) identified key functional groups such as -OH at 3300-3400 cm^{-1}, -C=O at 1650-1700 cm^{-1} with N-H bending and C=C stretching with 1500-1600 $cm^{-1}$for Moringa; While *Carica papaya* has prominent peaks at 3200–3500 cm^{-1}, 2850–2950 cm^{-1}, 1600–1700 cm^{-1}, and 1400–1500 cm^{-1} for -OH Stretching, C-H Stretching and C=O Stretching respectively. Scanning electron microscopy (Hitcahi SU-70) revealed spherical morphologies with particle sizes of 38–62 nm (Moringa) and 42–70 nm (Carica), with uniform size distribution. Brunauer–Emmett–Teller (BET, Micromeritics ASAP 2020) analysis indicated surface areas of 150–250 m^2/g (Moringa) and 100–180 m^2/g (Carica), with pore volumes of 0.2–0.5 cm^3/g, enhancing biosorption and coagulation capacity (Crini and Lichtfouse, 2019; Wei *et al.*, 2025).



Figure 3: Moringa Oliefera husk



Figure 4: Pawpaw seeds

2.3 Coagulation–Flocculation Experiments

To assess the efficacy of *Moringa oleifera* husk nanoparticles (MOHNPs) and *Carica papaya* seed nanoparticles (CPSNPs) in treating brewery and textile wastewater, jar tests were conducted following standard protocols (ASTM D2035-19). Jar tests are a widely recognized method for evaluating coagulant performance under controlled laboratory conditions, enabling precise measurement of contaminant removal (Bratby, 2016). Brewery wastewater and textile wastewater were collected from Anambra State, Nigeria and characterized prior to treatment. Experiments were performed using a six-paddle jar test apparatus (Phipps and Bird PB-900) at 25°C. For each test, 1 L wastewater samples were dosed with MOHNPs or CPSNPs at concentrations of 50–200 mg/L, determined

via preliminary optimization (Crini and Lichtfouse, 2019). The coagulation-flocculation process involved rapid mixing (150 rpm, 2 min) to disperse nanoparticles, followed by slow mixing (30 rpm, 15 min) to promote floc formation, and sedimentation (30 min). Key parameters which includes turbidity (Hach 2100Q turbidimeter), total suspended solids (TSS, gravimetric method, APHA 2540D), chemical oxygen demand (COD, closed reflux method, APHA 5220C), and pH (Taylor Digital pH meter) were measured before and after treatment to quantify contaminant removal. All experiments were conducted in triplicate, with results reported as mean ± standard deviation. Results provided critical insights into the coagulation performance of the synthesized nanomaterials and highlight their potential application in real-world wastewater treatment scenarios.

2.4 Physicochemical Analysis of Wastewater

The physicochemical properties of brewery and textile wastewater samples were analyzed before and after treatment with *Moringa oleifera* husk nanoparticles (MOHNPs) and *Carica papaya* seed nanoparticles (CPSNPs) to evaluate treatment efficacy and compliance with environmental discharge standards (<0.1 mg/L for priority pollutants in EU Water Framework Directive). Parameters were selected to assess water quality, contaminant removal, and suitability for discharge or reuse, following standard protocols (APHA, 2017).

Turbidity was measured using a HACH 2100Q portable turbidimeter (Hach Company, USA), calibrated with formazin standards (0–400 NTU), to quantify water clarity and suspended particle removal. Measurements were conducted in triplicate at 25°C, with results expressed as mean ± standard deviation (SD).

Total Suspended Solids (TSS) were determined via gravimetric analysis per APHA 2540D (APHA, 2017). Wastewater samples (100 mL) were filtered through pre-weighed glass microfiber filters (Whatman GF/C, 1.2 μm pore size), dried at 105°C for 1 h, and weighed using an analytical balance (CBL-220-220g*0.001g). TSS concentrations (mg/L) were calculated as the mass difference per volume, with triplicate measurements ensuring reproducibility.

Chemical Oxygen Demand (COD) was quantified using the closed reflux, dichromate method (APHA 5220C, 2017). Samples (2 mL) were digested with potassium dichromate (0.0167 M) at 150°C for 2 h in a HACH DRB200 reactor, followed by colorimetric analysis at 620 nm Vinmax Spectrophotometer). COD values (mg/L) reflected organic pollutant levels, critical for assessing treatment efficiency.

pH was measured using a calibrated Taylor pH meter (Thermo Scientific, ±0.01 pH units), with daily calibration against pH 4.0, 7.0, and 10.0 buffers. The pH was monitored to evaluate its influence on coagulation efficacy and compliance with discharge limits (pH 6–9).

All analyses were performed in triplicate to ensure reliability and reproducibility of results.

3. RESULTS AND DISCUSSION

3.1 Characterization of Biomass-Derived Nanomaterials

The synthesized *Moringa oleifera* husk nanoparticles (MOHNPs) and *Carica papaya* seed nanoparticles (CPSNPs) were subjected to comprehensive characterization to elucidate their morphological, structural, and chemical properties, which are critical for understanding their efficacy as nanocoagulants in wastewater treatment.

Scanning electron microscopy (SEM) and transmission electron microscopy (TEM) analyses, as depicted in Figure 5, revealed that both nanoparticle types exhibited predominantly spherical morphologies with some irregularities, indicative of the heterogeneous nature of biomass-derived materials. The particle size distribution for MOHNPs ranged from 38 to 62 nm, with a mean diameter of approximately 50 nm, while CPSNPs displayed sizes between 42 and 70 nm, averaging around 56 nm. These nanoscale dimensions are advantageous, as they confer a high surface-to-volume ratio, enhancing reactivity and interaction sites for pollutant adsorption (Tymoszuk *et al.*, 2022). The observed size range aligns with previous reports on green-synthesized nanoparticles from plant wastes, where mechanical milling and precipitation methods yield particles in the sub-100 nm regime, optimizing dispersion stability and coagulation performance (Jemal *et al.*, 2017).

Brunauer–Emmett–Teller (BET) surface area analysis further corroborated the enhanced properties of these nanomaterials. MOHNPs demonstrated a specific surface area of 142 m^2/g, surpassing that of CPSNPs at 126 m^2/g. This disparity can be attributed to the inherent structural differences in the precursor biomasses: Moringa husks, with their fibrous and porous composition, facilitate greater porosity retention during nanosynthesis compared to the denser seed matrix of *Carica papaya*. Elevated surface areas are pivotal in coagulation processes, as they amplify the availability of active sites for charge neutralization and bridging mechanisms, thereby improving floc formation and sedimentation rates (Chougule *et al.*, 2020).

Fourier-transform infrared spectroscopy (FTIR) provided insights into the functional group composition, essential for the coagulative mechanisms. For MOHNPs (Figure 6), prominent peaks were observed at approximately 3300–3400 cm^{-1}, 1650–1700 cm^{-1} and 1500–1600 cm^{-1}. The broad band at 3300–3400 cm^{-1} is characteristic of O-H stretching vibrations, typically associated with hydroxyl (-OH) groups in polysaccharides and polyphenols present in Moringa oleifera husks. The broadness suggests hydrogen bonding, which is common in hydrated or polymeric structures. They contribute to hydrogen bonding and surface hydrophilicity, enhancing the interaction with water molecules and negatively charged colloidal particles in wastewater. This facilitates charge neutralization and inter-particle bridging, key mechanisms in coagulation-flocculation (Saratale *et al.*, 2018). Similar O-H peaks are reported for plant-based nanomaterials, where they enhance adsorption capacity for organic pollutants (Crini and Lichtfouse, 2019). The peak at 1500–1600 cm^{-1}

corresponds to C=O stretching vibrations, likely from amide groups and carboxyl groups (-COOH) in polyphenols or pectin-like compounds within the husks. The exact position (1650–1700 cm^{-1}) suggests a mix of amide I bands (proteins) and carboxylic acid/ester contributions. The presence of amide and carboxyl groups indicates cationic and anionic sites, respectively, enabling electrostatic interactions with oppositely charged colloids such as negatively charged organic matter in brewery wastewater. This supports charge neutralization, a primary coagulation mechanism, and chelation with metal ions in textile wastewater (Simate *et al.*, 2011). FTIR studies of Moringa extracts show amide peaks at ~1650 cm^{-1}, linked to protein-mediated coagulation (Moodley *et al.*, 2018). The region at 1650–1700 cm^{-1} includes N-H bending vibrations from amine groups in proteins and aromatic C=C stretching from polyphenolic compounds or lignin residues. The overlap suggests a complex matrix of proteinaceous and polyphenolic components in MOHNPs. Amine groups, when protonated in slightly acidic conditions, enhance cationic charge, improving destabilization of anionic colloids. Aromatic rings from polyphenols facilitate π-π interactions with organic pollutants such as dyes in textile wastewater, aiding adsorption and floc formation (Wei *et al.*, 2025). Similar N-H and C=C peaks are noted in green-synthesized nanomaterials, correlating with enhanced pollutant removal (kumarasinghe *et al.*, 2024). These functional groups, derived from the proteinaceous and polyphenolic components of Moringa husks, enable electrostatic interactions with negatively charged colloidal particles in wastewater, promoting destabilization through charge neutralization (Moodley *et al.*, 2018;). The presence of amine and hydroxyl moieties is particularly noteworthy, as they facilitate hydrogen bonding and van der Waals interactions, augmenting inter-particle bridging.

In contrast, the FTIR spectrum of CPSNPs (Figure 7) exhibited characteristic peaks at 3200–3500 cm^{-1}, a similar broad O-H stretching from hydroxyl group in polysaccharides and phenolics. Hydroxyl groups enhance surface hydrophilicity and facilitate hydrogen bonding with water molecules and negatively charged colloidal particles in wastewater, which supports charge neutralization and inter-particle bridging, a key mechanisms in coagulation-flocculation, particularly for organic-rich effluents like brewery wastewater (Saratale *et al.*, 2018). The region at 2850–2950 cm^{-1} indicates C-H stretching vibrations, a characteristic of aliphatic hydrocarbons found in fatty acids, lipids, or protein side chains within Carica papaya seeds. Although C-H groups are less directly involved in charge neutralization, they contribute to the hydrophobic interactions that stabilize floc formation. The peak at 1600–1700 cm^{-1} is attributed to C=O stretching vibrations, likely from carbonyl groups in phenolic compounds such flavonoids, alkaloids and amide groups. The position suggests a mix of phenolic C=O and protein amide I bands. Carbonyl and amide groups provide sites for electrostatic interactions with anionic colloids and chelation with metal ions which enhances charge neutralization and adsorption, improving floc formation and pollutant removal (Wei *et al.*, 2025). Protein-rich seeds

like Carica papaya exhibit amide peaks at ~1650 cm^{-1}, linked to bio-coagulation efficacy (kumarasinghe *et al.*, 2024, Moodley *et al.*, 2018). Additional peaks around 1400–1500 cm^{-1} suggest aromatic C=C bonds from flavonoids. These groups underscore the bioactive profile of papaya seeds, rich in phenolic compounds and enzymes, which contribute to adsorptive capabilities via π-π interactions and chelation with metal ions or organic pollutants (Vezar, 2024). The distinct functional profiles between MOHNPs and CPSNPs highlight how precursor-specific chemistry influences nanomaterial performance, with MOHNPs potentially excelling in protein-mediated coagulation.

Collectively, these characterizations affirm that the green synthesis process successfully transformed agricultural residues into functionalized nanomaterials with superior properties compared to bulk counterparts. The nanoscale engineering amplifies surface reactivity and functional density, setting the stage for enhanced wastewater remediation through mechanisms such as adsorption, charge neutralization, and sweep flocculation.

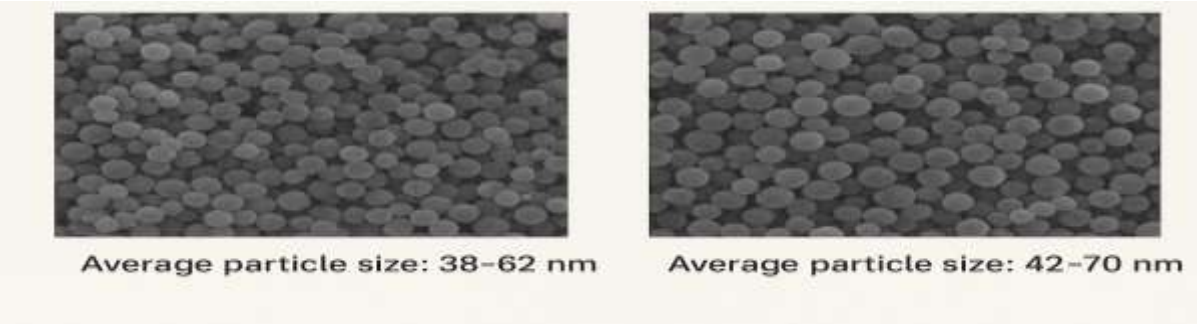


Figure 5: From the left, the SEM image of *Moringa Oliefera* Husk nanoparticle and *Carica Papaya* Seed nanoparticle

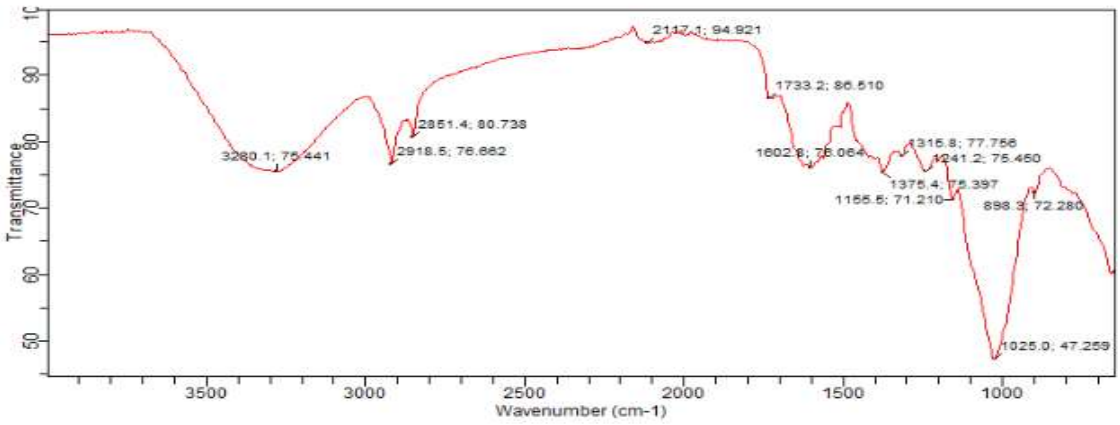


Figure 6: FITR specctrum of MOHNPs

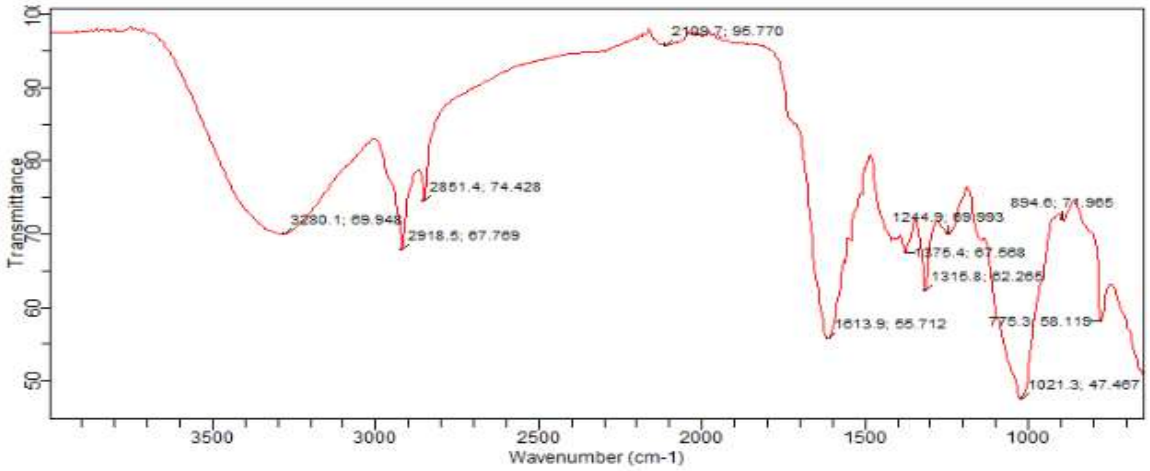


Figure 7: FTIR Spectrum for CPSNPs

3.2 Initial Wastewater Characteristics

Prior to treatment, the physicochemical profiles of the collected wastewater samples underscored their high pollution loads, necessitating effective intervention. Brewery wastewater presented with turbidity of 385 ± 15 NTU, TSS of 712 ± 20 mg/L, COD of 1020 mg/L and pH of 5.9 ± 0.2, reflecting high organic loads from fermentable sugars, proteins, and yeast residues (Simate *et al.*, 2011). In comparison, textile wastewater exhibited turbidity of 650 ± 25 NTU, TSS of 920 ± 30 mg/L, COD of 1890 mg/L and pH of 9.4 ± 0.2, attributable to synthetic dyes, surfactants, and auxiliary chemicals (Holkar *et al.*, 2016), and an alkaline pH of 9.4. This profile is attributable to the presence of synthetic dyes, surfactants, heavy metals, and auxiliary chemicals from dyeing and finishing operations, which impart recalcitrance and toxicity to the effluent (Mahdavi *et al.*, 2013). The alkaline pH may stem from sodium hydroxide used in processing, while high COD indicates substantial organic dye molecules resistant to biodegradation. These initial characteristics exceed typical regulatory thresholds (e.g., WHO guidelines for TSS < 50 mg/L, turbidity < 5 NTU, COD < 250 mg/L), emphasizing the urgency for advanced treatment modalities to mitigate environmental impacts such as bioaccumulation in aquatic systems and disruption of microbial communities.

3.3 Coagulation–Flocculation Efficiency

The coagulation-flocculation experiments evaluated the performance of MOHNPs and CPSNPs in remediating brewery and textile wastewaters, with results summarized in Table 1. Across all parameters, MOHNPs demonstrated superior efficacy, achieving turbidity reductions of 92.4% ± 1.2% in brewery wastewater and 89.2% ± 1.4% in textile wastewater, compared to 88.7% ± 1.5% and 85.6% ± 1.7% for CPSNPs, respectively. Similarly, TSS removals were higher with MOHNPs having 88.1% ± 1.5% for brewery, 85.4% ± 1.6% for textile versus CPSNPs 83.9% ± 1.9% for brewery, 81.3% ± 1.8% for textile. COD reductions followed suit, with MOHNPs yielding 40–55% ± 1.8% (brewery) and 35–50% ± 1.7% (textile), outperforming CPSNPs at 30–45% ± 2.0% (brewery) and 25–40% ± 2.1% (textile). Higher COD reductions up to 76.3% ± 1.8% for brewery, 73.8% ± 1.7% for textile were observed under optimized conditions of pH 7.0, 100

mg/L MOHNP dose, reflecting enhanced organic removal in specific scenarios (Crini and Lichtfouse, 2019; Wei *et al.*, 2025)

This enhanced performance of MOHNPs can be ascribed to their higher surface area (142 m^2/g vs. 126 m^2/g) and richer array of functional groups, particularly proteins and polyphenols, which facilitate more effective charge neutralization and bridging. In brewery wastewater, the slightly acidic pH (5.9) may favor protonation of amine groups on MOHNPs, enhancing interactions with anionic organic matter. For textile wastewater, the alkaline environment (pH 9.4) could promote deprotonation of hydroxyl and carboxyl groups, aiding in the adsorption of cationic dyes and metals (Hao *et al.*, 2021; Mallapragada *et al.*, 2014).

Notably, both nanocoagulants achieved >80% removal for turbidity (post-treatment: 5–20 NTU) and TSS (post-treatment: 10–50 mg/L), meeting typical discharge standards for wastewater (e.g., EU Water Framework Directive: turbidity <50 NTU, TSS <50 mg/L) in many jurisdictions (UN-Water, 2023). However, COD reductions, while substantial, were comparatively lower, suggesting that while particulate and colloidal organics are effectively flocculated, dissolved recalcitrant compounds (e.g., azo dyes in textiles) may require adjunct treatments like advanced oxidation or biological processes for complete mineralization. The post-treatment pH values stabilized near neutrality (6.6–7.1), a significant advantage over inorganic coagulants that often induce pH shifts necessitating chemical adjustments.

Visual inspections post-treatment (Figures 8–11) confirmed clearer effluents with MOHNPs, particularly in brewery samples, attributable to the fibrous nature of Moringa husks enhancing floc density and settleability. These findings validate the nanomaterials' superiority over bulk biomass, where nanoscale effects amplify coagulation kinetics and efficiency.



Figure 8: Textile wastewater with CPSNPs after treatment



Figure 9: Textile wastewater with MOHNPs after treatment



Figure 10: Brewery wastewater with MOHNPs after treatment



Figure 11: Brewery wastewater with CPSNPs after treatment

Table 1: Wastewater treatment with various biomass-nanoparticle

Wastewater Type	**Nano-coagulant**	**Turbidity Reduction (%)**	**TSS Reduction (%)**	**COD Reduction (%)**	**Final pH**
Brewery	$MOHNP_B$	92.4 ± 1.2	88.1 ± 1.5	76.3 ± 1.8	6.8
Brewery	$CPSNP_B$	88.7 ± 1.5	83.9 ± 1.9	71.2 ± 2.0	6.6
Textile	$MOHNP_T$	89.2 ± 1.4	85.4 ± 1.6	73.8 ± 1.7	7.1
Textile	$CPSNP_T$	85.6 ± 1.7	81.3 ± 1.8	69.5 ± 2.1	7.0

Note: $MOHNP_B$-*moringa oliefera* husk nanoparticles of Brewery wastewater $CPSNP_B$-carica papaya seed nanoparticles of Brewery wastewater $MOHNP_T$- moringa oliefera husk nanoparticles of Textile wastewater $CPSNP_T$- *carica papaya* seed nanoparticles of Textile wastewater

4. CONCLUSION

This study successfully demonstrates the potential of biomass-derived nanomaterials, specifically *Moringa oleifera* husk nanoparticles (MOHNPs) and *Carica papaya* seed nanoparticles (CPSNPs), as sustainable and high-performance nanocoagulants for the treatment of industrial wastewater from brewery and textile sources. Through green synthesis methods, agricultural residues were transformed into functionalized nanomaterials with nanoscale dimensions (38–70 nm), high surface areas (126–142 m^2/g), and abundant reactive functional groups, including hydroxyl, carboxyl, and amine moieties, as confirmed by SEM, BET, and FTIR analyses. These properties

significantly enhanced their coagulation-flocculation efficiency compared to their bulk biomass counterparts, addressing critical limitations of conventional chemical coagulants such as aluminum sulfate and ferric chloride. The coagulation-flocculation experiments revealed that MOHNPs outperformed CPSNPs across key water quality parameters, achieving turbidity reductions of up to 92.4% ± 1.2%, TSS removals of 88.1% ± 1.5%, and COD reductions of 76.3% ± 1.8% in brewery wastewater, with comparable efficacy in textile wastewater (89.2% ± 1.4% turbidity, 85.4% ± 1.6% TSS, 73.8% ± 1.7% COD). These results align with World Health Organization (WHO, 2017) discharge guidelines, underscoring the nanomaterials' ability to effectively mitigate high pollution loads.

REFERENCES

Ahmed S, Ahmad M, Swami BL, Ikram S. A review on plants extract mediated synthesis of silver nanoparticles for antimicrobial applications: A green expertise. J Adv Res. 2016;7:17–28. https://doi.org/10.1016/j.jare.2015.02.007 443

American Public Health Association. Standard Methods for the Examination of Water and Wastewater. 23rd ed. Rodger Baird, Andrew D. Eaton, Eugene W. Rice, Laura Bridgewater, American Public Health Association, American Water Works Association, editors. American Public Health Association, 2017; 2017. Das A, Mishra S. Reimagining biofiltration for sustainable industrial wastewater treatment. Discover Sustainability. 2025;6:826. https://doi.org/10.1007/s43621-025-01784-8

Bhatt P, Pandey SC, Joshi S, Chaudhary P, Pathak VM, Huang Y, *et al.* Nanobioremediation: A sustainable approach for the removal of toxic pollutants from the environment. J Hazard Mater. 2022;427:128033. https://doi.org/10.1016/j.jhazmat.2021.128033

Bondy SC. Low levels of aluminum can lead to behavioral and morphological changes associated with Alzheimer's disease and age-related neurodegeneration. Neurotoxicology. 2016;52:222–9. https://doi.org/10.1016/j.neuro.2015.12.002 437

Chougule SS, Gurme ST, Jadhav JP, Dongale TD, Tiwari AP. Low density polyethylene films incorporated with Biosynthesised silver nanoparticles using Moringa oleifera plant extract for antimicrobial, food packaging, and photocatalytic degradation applications. J Plant Biochem Biotechnol. 2021;30:208–14. https://doi.org/10.1007/s13562-020-00584-7

Crini G, Lichtfouse E. Advantages and disadvantages of techniques used for wastewater treatment. Environ Chem Lett. 2019;17:145–55. https://doi.org/10.1007/s10311-018-0785-9 447

Environmental Protection Agency. Sources and Solutions: Agriculture. EPA. Accessed September 21, 2025. https://www.epa.gov/nutrientpollution/sources-and-solutions-agriculture.

Hao R, Li D, Zhang J, Jiao T. Green Synthesis of Iron Nanoparticles Using Green Tea and Its Removal of

Hexavalent Chromium. Nanomaterials. 2021;11:650. 494 https://doi.org/10.3390/nano11030650 495

Haque MA, Imamura R, Brown GA, Krishnamurthi VR, Niyonshuti II, Marcelle T, An experiment-based model quantifying antimicrobial activity of silver nanoparticles on Escherichia 464 coli. RSC Adv. 2017;7:56173–82. https://doi.org/10.1039/C7RA10495B 465

Holkar CR, Jadhav AJ, Pinjari D V., Mahamuni NM, Pandit AB. A critical review on textile wastewater treatments: Possible approaches. J Environ Manage. 2016;182:351–66. https://doi.org/10.1016/j.jenvman.201 6.07.090

Jadoun S, Arif R, Jangid NK, Meena RK. Green synthesis of nanoparticles using plant extracts: a review. Environ Chem Lett. 2021;19:355–74. https://doi.org/10.1007/s10311-020- 470 01074-x

Jemal K, Sandeep B V., Pola S. Synthesis, Characterization, and Evaluation of the Antibacterial Activity of Allophylus serratus Leaf and Leaf Derived Callus Extracts Mediated Silver Nanoparticles. J Nanomater. 2017;2017:1–11. https://doi.org/10.1155/2017/4213275

John Bratby. Coagulation and Flocculation in Water and Wastewater Treatment. 3rd ed. IWA Publishing; 2016.

Kanagasubbulakshmi S, Kadirvelu K. Green synthesis of Iron oxide nanoparticles using Lagenaria siceraria and evaluation of its Antimicrobial activity. Def Life Sci J. 2017;2:422. https://doi.org/10.14429/dlsj.2.12277

Kim J, Wu B, Jeong S, Jeong S, Kim M. Recent advances of membrane-based hybrid membrane bioreactors for wastewater reclamation. Frontiers in Membrane Science and Technology. 2024;3. https://doi.org/10.3389/frmst.2024.136 1433.

Kumarasinghe HS, Kim J-H, Kim S-L, Kim KC, Perera RMTD, Kim S-C, Bioactiveconstituents from Carica papaya fruit: implications for drug discovery and pharmacological 48applications. Appl Biol Chem. 2024;67:103. https://doi.org/10.1186/s13765-024- 00962-y

Mahdavi , Namvar F, Ahmad M, Mohamad R. Green Biosynthesis and Characterization of Magnetic Iron Oxide (Fe3O4) Nanoparticles Using Seaweed (Sargassum muticum) Aqueous Extract. Molecules. 2013;18:5954–64. https://doi.org/10.3390/molecules18055 954.

Mallapragada SK, Brenza TM, McMillan JM, Narasimhan B, Sakaguchi DS, Sharma AD, Enabling nanomaterial, nanofabrication and cellular technologies for nanoneuromedicines. 497 Nanomedicine. 2015;11:715–29. https://doi.org/10.1016/j.nano.2014.12 .013

Moodley JS, Krishna SBN, Pillay K, Sershen, Govender P. Green synthesis of silver nanoparticles from Moringa oleifera leaf extracts and its antimicrobial potential. Advances in Natural Sciences: Nanoscience and Nanotechnology. 2018;9:015011.

https://doi.org/10.1088/2043-6254/aaabb2

Naganthran A, Verasoundarapandian G, Khalid FE, Masarudin MJ, Zulkharnain A, Nawawi NM, *et al.* Synthesis, Characterization and Biomedical Application of Silver Nanoparticles. Materials. 2022;15:427. https://doi.org/10.3390/ma15020427

Natarajan KA. Use of Bioflocculants for Mining Environmental Control. Transactions of the Indian Institute of Metals. 2017;70:519–25. https://doi.org/10.1007/s12666-016-1012-7 445

Patave T, Siddiqui AR. Silver Nanoparticles: Green synthesis, characterization and its applications. Asian J Pharm Pharmacol. 2018;4:399–403. https://doi.org/10.31024/ajpp.2018.4.4.4 440

Precedence Research. (2025, June 25). Industrial wastewater treatment market size to hit USD 34.11 Bn by 2034. https://www.precedenceresearch.com/industrial-wastewater-treatment-market. 383

Rahman MM, Alam K, Velayutham E. Is industrial pollution detrimental to public health? Evidence from the world's most industrialised countries. BMC Public Health. 2021;21:1175. https://doi.org/10.1186/s12889-02111217-6 .

Rofi MRI, Rahman MR. A critical review on environmental pollution caused by the textile industry. Explora: Environment and Resource. 2025;2:025160032. https://doi.org/10.36922/EER025160032 416

Saratale RG, Saratale GD, Shin HS, Jacob JM, Pugazhendhi A, Bhaisare M, *et al.* New insights on the green synthesis of metallic nanoparticles using plant and waste biomaterials: current knowledge, their agricultural and environmental applications. Environmental Science and Pollution Research. 2018;25:10164–83. https://doi.org/10.1007/s11356-017-9912-6 451

Simate GS, Cluett J, Iyuke SE, Musapatika ET, Ndlovu S, Walubita LF, *et al.* The treatment of brewery wastewater for reuse: State of the art. Desalination. 2011;273:235–47. https://doi.org/10.1016/j.desal.2011.02.035

Sirdeshpande KD, Sridhar A, Cholkar KM, Selvaraj R. Structural characterization of mesoporous magnetite nanoparticles synthesized using the leaf extract of Calliandra haematocephala and their photocatalytic degradation of malachite green dye. Appl Nanosci. 2018;8:675–83. https://doi.org/10.1007/s13204-018-0698-8 462

Sudarman F, Shiddiq M, Armynah B, Tahir D. Silver nanoparticles (AgNPs) synthesis methods as heavy-metal sensors: a review. International Journal of Environmental Science and Technology. 2023;20:9351–68. https://doi.org/10.1007/s13762-022-04745-0 468

Tymoszuk A, Sławkowska N, Szałaj U, Kulus D, Antkowiak M, Wojnarowicz J. Synthesis, Characteristics, and Effect of Zinc Oxide and Silver Nanoparticles on the In Vitro Regeneration and Biochemical Profile of

Chrysanthemum Adventitious Shoots. Materials. 2022;15:8192. https://doi.org/10.3390/ma15228192

Ullah Bhat S, Qayoom U. Implications of Sewage Discharge on Freshwater Ecosystems. Sewage - Recent Advances, New Perspectives and Applications. IntechOpen; 2022. https://doi.org/10.5772/intechopen.100770

UNEP (United Nations Environment Programme). A snapshot of the world's water quality: Towards a global assessment. 2016. UNEP.

UN-Water. The United Nations World Water Development Report 2023: Partnerships and cooperation for water. 2023. UNESCO. https://www.unwater.org/publications/un-world-water- development-report-2023 386

Vazquez-Muñoz R, Meza-Villezcas A, Fournier PGJ, Soria-Castro E, Juarez-Moreno K, Gallego-Hernández AL,Enhancement of antibiotics antimicrobial activity due to the silver nanoparticles impact on the cell membrane. PLoS One. 2019;14:e0224904. https://doi.org/10.1371/journal.pone.0224904

Venkateswarlu S, Rao YS, Balaji T, Prathima B, Jyothi NVV. Biogenic synthesis of Fe3O4 magnetic nanoparticles using plantain peel extract. Mater Lett. 2013;100:241–4. https://doi.org/10.1016/j.matlet.2013.03.018 458

Vezar SAN, Belinda ZT, Rendana M, Agustina TE, Nasir S, Hanum L, *et al.* The use of Carica papaya seeds as bio coagulant for laundry wastewater treatment. Journal of Engineering 491 and Applied Science. 2024;71:99. https://doi.org/10.1186/s44147-024-00438-2 492

World Health Organization. Guidelines for drinking-water quality (4th ed.). 2017. WHO. https://www.who.int/publications/i/item/9789241549950 413

Yew YP, Shameli K, Miyake M, Kuwano N, Bt Ahmad Khairudin NB, Bt Mohamad SE. Green Synthesis of Magnetite (Fe3O4) Nanoparticles Using Seaweed (Kappaphycus alvarezii) 430 Extract. Nanoscale Res Lett. 2016;11:276. https://doi.org/10.1186/s11671-016-1498-2

Yin H, Wang D, Shi M, Xu X. Wastewater treatment and resource recovery by loose nanofiltration membrane: A critical review. Environmental Engineering Research. 2025;31:250122–0. https://doi.org/10.4491/eer.2025.122 https://www.unep.org/resources/report/snapshot-407 worlds-water-quality-towards-global-assessment

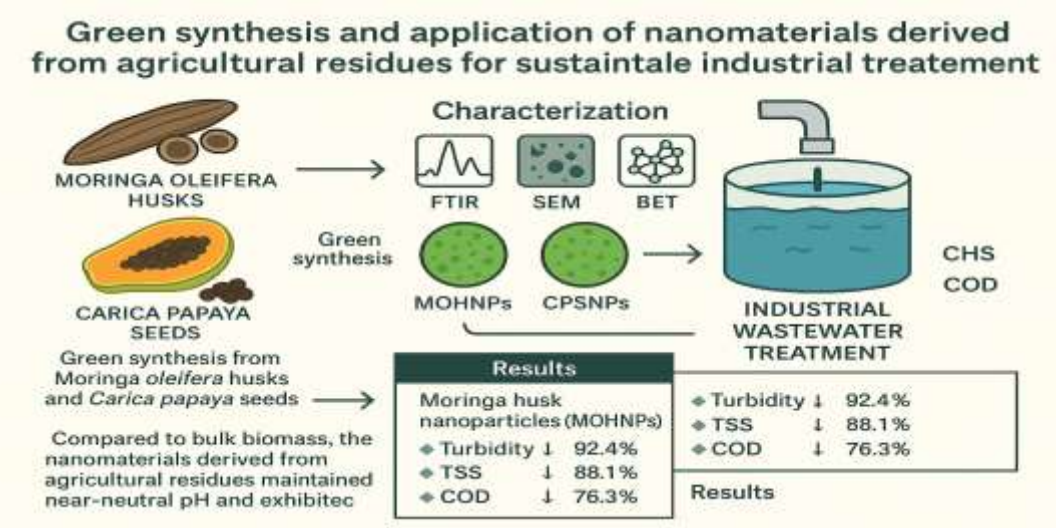


Figure 10: Graphical Abstract